15 May 2002

ELSEVIER

Optics Communications 206 (2002) 193–200

OPTICS COMMUNICATIONS

www.elsevier.com/locate/optcom

Design rules for dispersion-managed soliton systems

E. Poutrina *, Govind P. Agrawal

The Institute of Optics, University of Rochester, Rochester, NY 14627, USA

Received 26 September 2001; received in revised form 31 December 2001; accepted 2 January 2002

Abstract

We show that a limiting bit rate exists for dispersion-managed soliton systems and it depends only on the dispersion-map configuration. We introduce a new map parameter that determines the minimum input pulse width that can be launched into a dispersion-managed soliton system. We use this parameter to provide simple design rules and approximate analytic expressions for the three input pulse parameters (pulse width, chirp, and energy) for a two-fiber-section dispersion map and verify their accuracy numerically. The results confirm the known empirical result that pulse interactions are minimized for a map strength of about 1.6. They also explain why dense dispersion management is needed at high bit rates. © 2002 Published by Elsevier Science B.V.

1. Introduction

Dispersion management has proven to be an important technique as it can be used to lower the average dispersion of a fiber link even though the group-velocity dispersion (GVD) is kept relatively large locally for suppressing four-wave mixing. The use of dispersion-managed (DM) solitons provides a number of advantages over the conventional solitons occurring in constant-GVD fibers [1]. However, the design of DM soliton system requires a careful choice of input parameters (such as the pulse energy, width, and chirp) to ensure that each soliton recovers its input state after each map period. A variational technique is commonly used to find the periodic solutions of a dispersion map [2]. However, its use still requires a numerical approach. In this paper we propose simple design rules that can be quite beneficial in practice.

The paper is organized as follows. Section 2 outlines the variational approach. The resulting variational equations for the pulse width and chirp are solved numerically to show that a minimum value of the input pulse width exists for all maps. This minimum value is estimated in Section 3 by solving the variational equations approximately and is shown to depend on a single map parameter T_{map}. We use this parameter in Section 4 to provide a few simple design rules. The input pulse energy is estimated in Section 5. This approach allows us to find analytic expressions for the pulse energy, width, and chirp. The main results are summarized in Section 6.

* Corresponding author. Fax: +1-716-275-7834.
E-mail address: putrina@optics.rochester.edu (E. Poutrina).

0030-4018/02/$ - see front matter © 2002 Published by Elsevier Science B.V.
PII: S0030-4018(02)01391-3

2. Variational analysis

Pulse propagation in a DM lightwave system can be described by the following nonlinear Schrödinger equation [3]:

$$\mathrm{i}\frac{\partial A}{\partial z}-\frac{\beta_2}{2}\frac{\partial^2 A}{\partial t^2}+\gamma|A|^2A=-\frac{\mathrm{i}}{2}\alpha A, \tag{1}$$

where A is the pulse amplitude, β_2 is the GVD parameter, γ is a nonlinear coefficient, and α accounts for fiber losses and its periodic compensation through optical amplifiers. All three parameters are periodic functions of z for a DM system. The variational method solves Eq. (1) with the following ansatsz:

$$A(z,t)=\frac{\sqrt{E}}{\sqrt{\pi}T}\exp\left[(1+\mathrm{i}C)\frac{t^2}{2T^2}-\mathrm{i}\Omega t+\mathrm{i}\phi\right], \tag{2}$$

where $E\equiv E_0\mathrm{e}^{-\alpha z}$ is the energy, E_0 being the input energy of the pulse, T is the width, C is the chirp, Ω is the frequency shift, and ϕ is the phase of the pulse. All five parameters are periodic functions of z. In practice, Ω and ϕ can be chosen to be zero at $z=0$. However, the input values E_0, T_0, and C_0 of the remaining three parameters need to be specified to ensure periodic propagation of the input pulse through the dispersion map. The evolution of the pulse width $T(z)$ and the chirp $C(z)$ in each fiber section of a DM system is described by the following two coupled equations [1]:

$$\frac{\mathrm{d}T}{\mathrm{d}z}=\frac{\beta_2 C}{T}, \tag{3}$$

$$\frac{\mathrm{d}C}{\mathrm{d}z}=\frac{\gamma_0 E_0\exp(-\alpha z)}{\sqrt{2\pi}T}+\frac{\beta_2(1+C^2)}{T^2}. \tag{4}$$

The DM soliton corresponds to a solution of Eqs. (3) and (4) with the periodic boundary conditions: $T(0)=T(L_\mathrm{A})$ and $C(0)=C(L_\mathrm{A})$, L_A being the amplification period in the system.

Solving the above two variational equations numerically, we find periodic solutions over a relatively large range of input energy E_0. For illustration purposes, we focus on two kinds of maps that are used commonly in practice. Each map is made of two types of fibers with dispersions β_{21} and β_{22} and lengths l_1 and l_2. The map A consists of dispersion-shifted and reverse-dispersion fibers of nearly equal length ($l_1\approx l_2=5$ km) with $\beta_{21}=-\beta_{22}=-4$ ps^2/km. The map B is made using standard (SMF) fiber of 60-km length ($\beta_{21}=-22$ ps^2/km) and dispersion-compensating fiber of about 14.5 km length ($\beta_{21}=100$ ps^2/km). We adjust the average dispersion of the map in the range -0.005 ps^2/km to -0.15 ps^2/km by changing the length l_2. Although the nonlinear parameter γ is generally different for different types of fibers, in this work we use $\gamma=2.5$ W^{-1} km^{-1} unless stated otherwise. This choice does not affect our conclusions.

Fig. 1 shows the values of input pulse width as a function of E_0 for the dispersion map A with average dispersion $\overline{\beta}_2=-0.01$ ps^2/km. The curves marked "T_0" represent the input width while the curves "T_m" correspond to the minimum pulse width occurring in the fiber section with anomalous GVD. The inset shows the input chirp C_0 as a function of E_0. Solid curves in Fig. 1 represent the loss-less case ($\alpha=0$) and dashed curves correspond to a loss of 0.25 dB/km in each fiber section. We focus on the case of dense

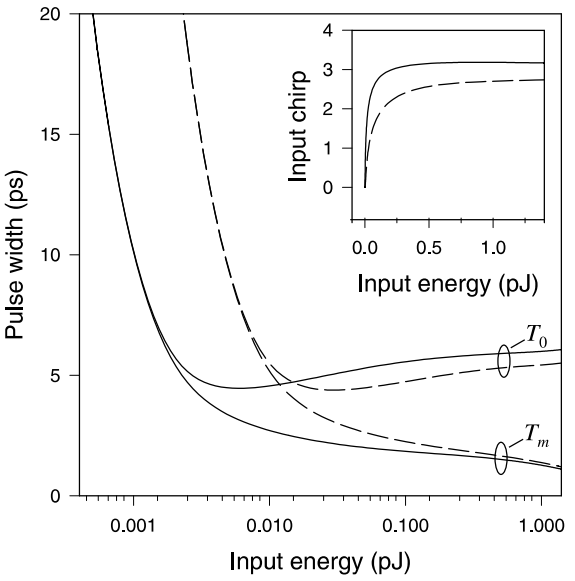

Fig. 1. Input pulse width T_0 and corresponding minimum pulse width T_m as a function of input energy E_0 for the map A with $\overline{\beta}_2=-0.01$ ps^2/km. The dependence of input and minimum pulse widths on the input energy value. Solid curves are for the loss-less case ($\alpha=0$), while $\alpha=0.25$ dB/km for dashed. The inset shows the input chirp in the two cases.

dispersion management [4–7] in the case of map A and assume that the amplification period L_A includes 8 map periods $L_m : L_A = 8L_m = 80$ km. We have verified that the input parameters shown in Fig. 1 lead to stable propagation of solitons over more that 10^5 km (in the absence of noise) when Eq. (1) is solved numerically by using the split-step method.

For low pulse energies, both T_0 and T_m decrease rapidly. Moreover, T_0 and T_m values nearly coincide, indicating that in this region pulse width does not oscillate and remains nearly equal to T_0. An important feature is that at some value of $E_0 = E_c$ the curve $T_0(E_0)$ has a minimum value T_0^{min}. When E_0 exceeds E_c, T_0 and T_m curves diverge from each other, and pulse width starts to oscillate more and more within each fiber section. The qualitative character of the curve $T_m(E_0)$ also changes around E_c from a rapid to a relatively slow decrease, while T_0 slowly increases. The qualitative features shown in Fig. 1 hold for any two-section dispersion map having negative $\overline{\beta}_2$.

Two parameters are especially important for DM solitons—the ratio $\overline{\beta}_2/\gamma$ [8] and the stretching factor S_t [9]. In place of the stretching factor we introduce a new parameter

$$T_{map} \equiv \left| \frac{\beta_{21}\beta_{22} l_1 l_2}{\beta_{21} l_1 - \beta_{22} l_2} \right|^{1/2}, \tag{5}$$

which depends only on the map parameters β_{2j} and l_j and has units of time. The use of this parameter is justified later. Fig. 2 shows variations of $T_0(E_0)$ and $T_m(E_0)$ for two values of the ratio $\overline{\beta}_2/\gamma$ and two values of T_{map}. Dispersion maps A (solid curves) and B (dashed curves), each with two different values of average dispersion ($\overline{\beta}_2 = -0.01$ and -0.15 ps^2/km) are used in this calculation. As we can see from the figure, the $\overline{\beta}_2/\gamma$ ratio affects dramatically the energy, at which T_0 takes its minimum value T_0^{min} (in agreement with the result of [8]), but it does not affect much the minimum value itself, or the range of pulse oscillations from T_0 to T_m. In contrast, the value of T_0^{min}, as well as the asymptotic value of T_m at large energies, depends only on the parameter T_{map}. These results show that for a given two-section map configuration, there exists a limiting bit rate that depends on the value of T_{map}.

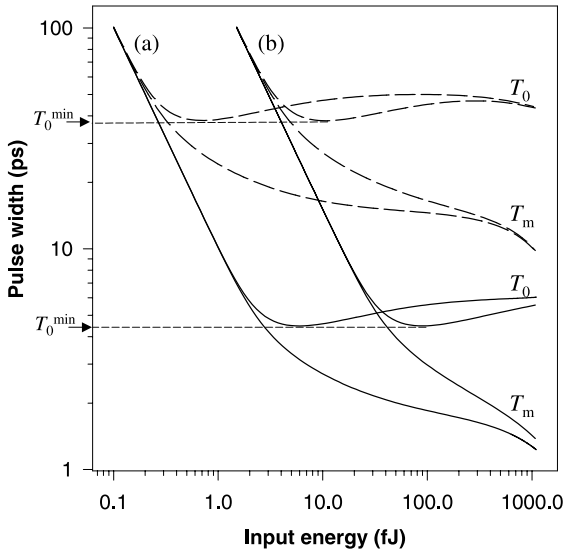

Fig. 2. Same as Fig. 1 except that two different values of $\overline{\beta}_2/\gamma$ are shown for two different maps: (a) $\overline{\beta}_2/\gamma = -0.004$ (ps^2 W), (b) $\overline{\beta}_2/\gamma = -0.06$ (ps^2 W). Solid curves are for map A ($T_{map} = 3.16$ ps) while dashed curves are for map B ($T_{map} = 26.9$ ps). Loss $\alpha = 0$ in all cases.

Considering a wide variety of dispersion maps with different values of $\overline{\beta}_2/\gamma$ and T_{map}, we find that for the loss-less case, the value of T_0^{min} always corresponds to $C_0 = \pm 1$ (the choice of sign depends on whether β_{21} is negative or positive, respectively). An important feature is that, in a large range of $\overline{\beta}_2$ values, not only the value of T_0^{min}, but the whole curve $T_0(C_0)$ is invariant with respect to the ratio $\overline{\beta}_2/\gamma$. In the next section we use this result and the qualitative features of Fig. 2 to find the dependence of T_0 on C_0 in an approximate analytic form.

3. Analytical estimate of T_0

We obtain an approximate analytic formula for the input pulse width in the loss-less case, setting $\alpha = 0$ in Eq. (4). This approach is justified because, as one can see from Fig. 1, T_0^{min} value and the range of pulse oscillations are almost the same in a DM system with no loss and in a DM system having 0.25 dB/km loss in each fiber section. This observation remains valid for systems with short-period dispersion maps, having any number of

map periods within the amplification period. In such systems, $T_0^{\min}$ also corresponds to $|C_0| \approx 1$ even in the presence of loss. This is the consequence of the fact that in short-period maps the chirp-free point is close to the middle of fiber segments even in the presence of losses (in the lossless case it is exactly in the middle [10]). The importance of this observation will become clear from what follows.

Eq. (3) can be integrated formally to find

$$T^2(z) = T_0^2(z) + 2\int_0^z \beta_2(z)C(z)\,\mathrm{d}z. \tag{6}$$

Thus, $T(z)$ can be determined if $C(z)$ is known. Since a closed form expression for $C(z)$ is not available, we follow an empirical method. Numerical simulations show that the chirp C can be represented, with an accuracy better than 0.1%, as a linear function of z in each fiber section for energy values in the range from 0 to about $5\hat{E}_0$. Using the fact that the chirp-free points are situated in the middle of each section for $\alpha = 0$ [10], we approximate the chirp in each map period as

$$C(z) = \begin{cases} C_0\left(1 - \frac{2}{l_1}z\right) & \text{if } 0 \leqslant z \leqslant l_1, \\ -C_0\left(1 - \frac{2}{l_2}(z - l_1)\right) & \text{if } l_1 \leqslant z \leqslant L_m. \end{cases} \tag{7}$$

Using Eq. (7) in Eq. (6), we obtain the following approximate expression for pulse width:

$$T^2(z) = \begin{cases} T_0^2 + 2\beta_{21}C_0\left(1 - \frac{z}{l_1}\right)z & \text{if } 0 \leqslant z \leqslant l_1, \\ T_0^2 - 2\beta_{22}C_0\left(1 - \frac{(z-l_1)}{l_2}\right)(z - l_1) & \text{if } l_1 \leqslant z \leqslant L_m. \end{cases} \tag{8}$$

In order to connect T_0 and C_0 values, we consider the ratio $(1 + C^2)/T^2$ because it represents the spectral width of a chirped pulse. In a linear system, this ratio remains constant and is equal to $1/T_{\mathrm{m}}^2$. Numerical simulation show, that this ratio does not change much with propagation even in a DM system when the nonlinear length [3] is much larger than the local dispersion length. More specifically, it oscillates within each map period around its average value $(1 + C_0^2)/T_0^2$ by less than 1%. Since the ratio $(1 + C^2)/T^2$ is almost constant during the propagation, the integral

$$I(z) \equiv \int_0^z \frac{1 + C^2(z')}{T^2(z')}\,\mathrm{d}z' \approx \frac{1 + C_0^2}{T_0^2}z, \tag{9}$$

grows almost linearly with z. We can estimate the error by calculating I using Eqs. (7) and (8). The result is found to be

$$I(z) = \begin{cases} -\frac{2C_0}{D_1 l_1}z + \varepsilon_1(z), & 0 \leqslant z \leqslant l_1, \\ I(l_1) + \frac{2C_0}{D_2 l_2}(z - l_1) + \varepsilon_2(z - l_1), & l_1 < z \leqslant L_m, \end{cases} \tag{10}$$

where $\varepsilon_i(z)$ $(i = 1, 2)$ is defined as

$$\varepsilon_i(z) \equiv -\frac{1}{2}\frac{a_i b_i - c_i}{\sqrt{c_i^3 b_i}}\left[\tan^{-1}\left(\sqrt{\frac{c_i}{b_i}}(l_i)\right) - \tan^{-1}\left(\sqrt{\frac{c_i}{b_i}}(l_i - 2z)\right)\right] \tag{11}$$

and a_i, b_i, c_i are given by

$$a_i \equiv \frac{C_0^2}{l_i^2}, \quad b_i \equiv \pm\frac{1}{2}\beta_{2i}C_0 l_i + T_0^2, \quad c_i \equiv \mp\frac{\beta_{2i}C_0}{2l_i}. \tag{12}$$

In (12), the upper and lower signs correspond to the first $(i = 1)$ and second $(i = 2)$ fiber sections, respectively. For all practical maps, ε_1 and ε_2 are found to be negligible. Numerical simulations also confirm that the error in Eq. (9) does not exceed 0.2%.

Neglecting ε_1 and ε_2 in Eq. (10), we notice that $I(z)$ varies linearly with z but with different slopes. Assuming that the average dispersion is relatively small, we find the average slope and equate it to $(1 + C_0^2)/T_0^2$ from Eq. (9). We then obtain the following expression for the input pulse width in terms of C_0 and dispersion-map parameters:

$$T_0 = T_{\mathrm{map}}\sqrt{\frac{1 + C_0^2}{|C_0|}}. \tag{13}$$

Note the appearance of a single map parameter T_{map} defined as in Eq. (5). This parameter has units of time and plays an important role in the following discussion. The dependence of input pulse width on the input chirp C_0 for the four DM systems of Fig. 2 is shown in Fig. 3. Open lines represent the values of input pulse width T_0 calculated

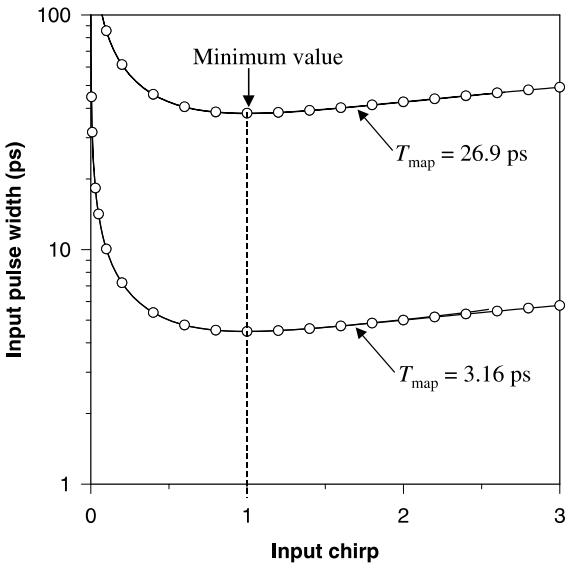

Fig. 3. Comparison of the input pulse width predicted by Eq. (13) (circles) with the numerically calculated values (solid curves) as a function of input chirp for the four maps of Fig. 2. Only two curves appear since results are nearly independent of the ratio $\overline{\beta}_2/\gamma$.

using Eq. (13), while solid circles show the results obtained by solving variational Eqs. (3) and (4) numerically. We find a very good agreement up to chirp values of $|C_0| = 3$. Although four dispersion maps are used for in Fig. 3, only two curves appear in this figure because, as was mentioned before, the dependence of $T_0(C_0)$ curve on the ratio $\overline{\beta}_2/\gamma$ is negligible when the average dispersion is much smaller than the local dispersion value. For that reason, the curves for $\overline{\beta}_2/\gamma = -0.004$ and $\overline{\beta}_2/\gamma = -0.06$ are indistinguishable in Fig. 3.

Eq. (13) can be used to find the minimum pulse width. Noticing that the chirp is zero at the location of the minimum pulse width point and using the fact that $(1 + C_0^2)/T_0^2 \approx 1/T_m^2$, the minimum pulse width is given by

$$T_m = \frac{T_{map}}{\sqrt{|C_0|}}. \tag{14}$$

Eq. (14) provides the average value of minimum pulse width in sections with positive and negative dispersions, but these values do not differ much in the region around $|C_0| \approx 1$. A comparison with numerical solutions shows that Eq. (14) is accurate to within 2% up to the values of input chirp $|C_0| \approx 3$. Several interesting conclusions can be drawn from Eqs. (13) and (14). First, the minimum value of the input pulse width from Eq. (13) indeed occurs for $|C_0| = 1$, as also found numerically. Second, when $|C_0| = 1$, T_m is just equal to the map parameter T_{map}. The input pulse width in this case is $T_0 = \sqrt{2}T_{map}$, showing that pulse width is stretched by the factor of $\sqrt{2}$ within each fiber link when input pulse width corresponds to its minimum width allowed for a given dispersion map.

4. Design rules

Eq. (14) shows that the qualitative change of the $T_m(E_0)$ curve in Figs 1 and 2 from a very rapid to a very slow decrease is due to $1/|C_0|$ dependence of the minimum pulse width. The value of $|C_0|$, as seen in the inset of Fig. 1, increases rapidly with increased energies. According to the above discussion, the map parameter T_{map} is an important design parameter for system characterization, since $\sqrt{2}T_{map}$ and T_{map} describe, respectively, the minimum possible input width and the corresponding shortest pulse width in the fiber link for a given dispersion map.

Eq. (13) provides the values of input pulse width as a function of input chirp. We now consider which range of input chirp values should be used to obtain the best pulse sequence propagation. From 1–3 we note that just after T_0 takes its minimum value, T_m continues to decrease while T_0 is relatively constant. We expect the longest propagation distance, as well as a highest bit rate for a given distance, to occur in this region ($|C_0| \gtrsim 1, E_0 \approx E_c$). For energies smaller than E_c, the bit rate is limited by the large values of T_0 and T_m, and for energies much larger than E_c it would be limited by pulse interactions because of increased pulse stretching and higher pulse energies. This is confirmed in Fig. 4, where we show the maximum propagation length as a function of input chirp C_0 for 80 and 160 Gb/s. The map with $\beta_{21} = 4$ ps^2/km and $\beta_{22} = -4$ ps^2/km is used in this calculation by choosing $\overline{\beta}_2 = -0.01$ and -0.005 ps^2/km for 80 and 160 Gb/s systems, respectively. We also reduce the section length to

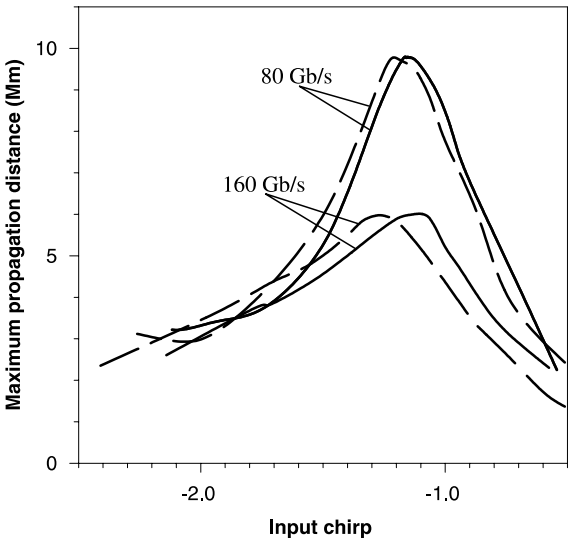

Fig. 4. Maximum propagation distance as a function of input chirp for systems operating at 80 and 160 Gb/s bit rates. Loss parameter $\alpha = 0$ for solid curves but $\alpha = 0.25$ dB/km for dashed curves.

$l_1 = 0.6$ km, for 160 Gb/s system, and use $l_1 = 3$ km for 80 Gb/s systems. The solid curves represent the results when losses are neglected and the dashed curves include 0.25 dB/km loss in each fiber section and assume 80 km amplifier spacing. Two points are noteworthy. First, maximum distance can exceed 6000 km even at 160 Gb/s when dense DM is used [11]. Second, in all cases the maximum occurs in the region $1.1 < |C_0| < 1.2$.

Eqs. (13) and (14) allow us to estimate the maximum possible bit rate for a given map configuration. For example, consider a dispersion map made using 70 km of standard fiber ($\beta_{21} = -22$ ps^2/km) and 15.3 km of DCF ($\beta_{22} = 100$ ps^2/km). The average dispersion for this map is $\overline{\beta}_2 \approx -0.1$ ps^2/km, while $T_{\text{map}} = 27.7$ ps. From Eqs. (14) and (13), T_{m} is about 26.4 ps and $T_0 \approx 39.3$ ps at $|C_0| = 1.1$, the chirp value within the optimum range. Since the shortest pulse width that can propagate as a DM soliton is 26.4 ps, such a map configuration can never provide a bit rate of 40 Gb/s for which the bit slot is only 25 ps. To increase the bit rate, according to Eqs. (13) and (14), one needs to reduce the value of the map parameter T_{map}. From Eq. (5) this is possible by reducing either the dispersion or the length of fiber segments.

Consider the design of a 160 Gb/s system. Since the bit slot is only 6.25 ps wide, the map parameter T_{map} should not exceed 1.06 ps to avoid soliton interaction. For $(\beta_{2i} - \overline{\beta}_2) = \pm 1$ ps^2/km ($i = 1$ and 2 in the first and second fiber sections, respectively), according to Eq. (5), we need to take $l_i \approx 2.24$ km. Moreover, the section lengths reduce to only $l_i \approx 0.6$ km if it is necessary to use larger local dispersion values of ± 4 ps^2/km to avoid four-wave mixing in WDM applications. This result explains why dense dispersion management is a necessity for designing systems at bit rates > 40 Gb/s [4–7].

We now discuss the range of map strength [8] S_{m} corresponding to the values of input chirp $1.1 < |C_0| < 1.2$. The map strength parameter in our notation can be written as

$$S_{\text{m}} = \frac{\left|(\beta_{21} - \overline{\beta}_2) l_1 - (\beta_{22} - \overline{\beta}_2) l_2\right|}{\left(1.665 T_{\text{map}}\right)^2} |C_0|, \tag{15}$$

where the factor of 1.665 results from using the full width at half maximum. For small average dispersion values, $|\beta_{21} l_1| \approx |\beta_{22} l_2|$, and Eq. (15) can be approximated as $S_{\text{m}} \approx 1.443 |C_0|$. As discussed above, pulse interactions are minimized for value of input chirp $|C_0|$ between 1.1 and 1.2. Using those values, we find that the least interactions occur for $1.59 \lesssim S_{\text{m}} \lesssim 1.73$, which agrees with the known empirical result that the least interactions occur for S_{m} values around 1.6 [9]. For a small average dispersion value, we can also approximate Eq. (13) as $T_0^2 \approx |\beta_{21} l_1| (1 + C_0^2)/(2|C_0|)$. Using $C_0 \approx 1.1$ and $L_{\text{D}} \equiv T_0^2/|\beta_{21}|$, the configuration giving the map strength of about 1.6 corresponds to the map for which the length of each fiber segment is approximately equal to the local dispersion length L_{D}.

Although Eqs. (13) and (14) appear similar to those obtained for a linear system, the presence of nonlinearity is critical for DM solitons. In fact, a periodic solution of Eqs. (3) and (4) does not exist in the linear case ($\gamma = 0$) unless the average dispersion $\overline{\beta}_2$ is zero. We have verified through numerical simulations that Eq. (13) remains valid in the region $1 \leqslant |C_0| \leqslant 1.5$ with an accuracy better

than 1% as long as the value of $\overline{\beta}_2 L_m$ does not exceed $\approx 12\%$ of $(\beta_{2i} - \overline{\beta}_2) l_i$ in the ith section ($i = 1, 2$). This relation gives, for example, average dispersion as large as $\overline{\beta}_2 = -0.5$ ps^2/km for $(\beta_{2i} - \overline{\beta}_2) l_i = 20$ ps^2 and $\overline{\beta}_2 \approx -2$ ps^2/km for $(\beta_{2i} - \overline{\beta}_2) l_i = 1500$ ps^2.

5. Input energy estimation

Eq. (13) provides the input pulse width corresponding to a given input chirp, while the full set of input parameters also includes the value of input energy E_0. In this section we estimate E_0 with the help of the approximate solution given in Eqs. (7) and (8). Setting $\alpha = 0$ in Eq. (4), integrating it over one map period and using the periodicity condition $C(0) = C(L_m)$ we obtain

$$\int_0^{L_m} \frac{\gamma_0 E_0}{\sqrt{2\pi} T} + \int_0^{L_m} \beta_2 \frac{1 + C^2}{T^2}\, dz = 0. \tag{16}$$

Using Eqs. (7) and (8) and performing the integration, we arrive at the following expression for the input energy:

$$E_0 = 2\sqrt{2\pi} \frac{\beta_{21}\varepsilon_1(l_1) + \beta_{22}\varepsilon_2(l_2)}{(\gamma_{01}/\sqrt{c_1}) \ln r_1 + (\gamma_{02}/\sqrt{c_2}) \ln r_2}, \tag{17}$$

where $r_i \equiv (T_0 - l_i\sqrt{c_i})/(T_0 + l_i\sqrt{c_i})$, γ_{0i} is the nonlinear coefficient in each fiber section ($i = 1, 2$), and ε_i and c_i are given by Eqs. (11) and (12). A comparison with numerical solutions of the variational equations shows that energy values obtained from Eq. (17) differ by at most 5% from numerically obtained values in the region around $|C_0| = 1$, while the difference becomes about 10% for $|C_0| \approx 1.25$. We have verified that energy values obtained using Eq. (16) give a stable pulse propagation up to about 40 Mm. Although the error in E_0 leads to larger peak power oscillations during propagation, the amplitude of the oscillations does not exceed $\pm 5\%$ of the average peak power. As discussed in [5], the input energy E_0 also depends on the ratio L_A/L_m and in general decreases as this ratio increases.

Note that Eq. (17) is derived for a loss-less system or for systems with distributed amplification. The effect of periodic gain/loss variation can be included by increasing E_0 by a factor of $G \ln G/(G - 1)$, where G is the amplifier gain [2]. This scaling is valid for values of S_m up to 4 for DM systems with short fiber sections.

6. Conclusions

We have shown that a limiting bit rate exists for DM systems and it depends only on the dispersion-map configuration. We have introduced a new map parameter that determines the minimum input pulse width that can be launched into the DM system. We use this parameter to provide simple design rules that can be used for estimating the limiting bit rate. Using the approximate analytic solutions of the variational equations, we have provided the input values of the three pulse parameters for a two-fiber-section dispersion map. We compared our approximate values of the input chirp, width, and energy with numerical solutions of the variational equations and found a very good agreement with the numerical results. Our results also help to explain why dense dispersion management is necessary for designing high-bit-rate DM systems.

Acknowledgements

This research is supported in part by the US National Science Foundation under grants ECS-9903580 and DMS-0073923.

References

[1] G.P. Agrawal, Applications of Nonlinear Fiber Optics, Academic Press, New York, 2001, Chapter 8.
[2] S.K. Turitsyn, E.G. Shapiro, Opt. Fiber Technol. 4 (1998) 151.
[3] G.P. Agrawal, Nonlinear Fiber Optics, third ed., Academic Press, New York, 2001, Chapters 2 and 5.
[4] A.H. Liang, H. Toda, A. Hasegawa, Opt. Lett. 24 (1999) 799.
[5] S.K. Turitsyn, M.P. Fedoruk, A. Gornakova, Opt. Lett. 24 (1999) 869.
[6] L.J. Richardson, W. Forysiak, N.J. Doran, Opt. Lett. 25 (2000) 1010.
[7] A. Maruta, Y. Yamamoto, S. Okamoto, A. Suzuki, T. Morita, A. Agata, A. Hasegawa, Electron. Lett. 36 (2000) 1947.

[8] N.J. Smith, N.J. Doran, F.M. Knox, W. Forysiak, Opt. Lett. 21 (1996) 1981.
[9] T. Yu, E.A. Golovchenko, A.N. Pilipetskii, C.R. Menyuk, Opt. Lett. 22 (1997) 793.
[10] S.K. Turitsyn, J.H.B. Nijhof, V.K. Mezentsev, N.J. Doran, Opt. Lett. 24 (1999) 1871.
[11] L.J. Richardson, W. Forysiak, N.J. Doran, IEEE Photon. Technol. Lett. 13 (2001) 209.